PHYSICAL REVIEW A, VOLUME 65, 042313

Coherent superposition states as quantum rulers

T. C. Ralph*
Centre for Quantum Computer Technology, Department of Physics, The University of Queensland, St. Lucia, QLD 4072, Australia
(Received 22 September 2001; published 1 April 2002)

We explore the sensitivity of an interferometer based on a quantum circuit for coherent states. We show that its sensitivity is at the Heisenberg limit. Moreover, we show that this arrangement can measure very small length intervals.

DOI: 10.1103/PhysRevA.65.042313 PACS number(s): 03.67.−a, 42.50.Dv

There exists a well-known isomorphism between interferometers and basic quantum processing circuits. In particular, the circuit comprising a Hadamard gate followed by a phase gate and then a second Hadamard gate is equivalent to a single photon, optical interferometer with a phase shift in one arm (see Fig. 1). Historically this observation has helped to identify candidate quantum circuits [1]. An alternative viewpoint is to consider the efficacy of such quantum circuits in performing more traditionally interferometric tasks [2–5].

We have recently proposed an efficient quantum computation scheme based on a coherent-state qubit encoding, conditioned linear optics, and coherent superposition state resources [6]. Here we investigate how sensitively distance measurements can be made using the equivalent of the circuit in Fig. 1(a) when realized using this scheme. We find that its sensitivity to small perturbations in length is at the Heisenberg limit. Further more we find that its sensitivity in measuring small *length intervals* is also at the Heisenberg limit. We refer to this effect as a *quantum ruler*.

Our logical qubits are encoded as follows: the zero state is the vacuum, $|0\rangle_L=|0\rangle$, and the one state is the coherent state of amplitude α, $|1\rangle_L=|\alpha\rangle$. We assume that the coherent amplitude is real and that $\alpha\gg1$. Note that this qubit encoding is distinct from other quantum circuit [7,8] and interferometric [9] proposals. We begin by investigating the sensitivity of the idealized circuit of Fig. 1(a) using our coherent-state qubit encoding and comparing this with the sensitivity of a standard interferometer with a squeezed vacuum input. We then introduce a physical realization of the quantum circuit and consider some more practical issues.

Consider the case of the logical zero state, i.e., the vacuum, entering the first Hadamard gate. The effect of a Hadamard gate is to produce the following transformations in the logical basis:

$$|0\rangle_L\rightarrow\frac{1}{\sqrt{2}}(|0\rangle_L+|1\rangle_L),$$

$$|1\rangle_L\rightarrow\frac{1}{\sqrt{2}}(|0\rangle_L-|1\rangle_L). \tag{1}$$

*Email address: ralph@physics.uq.edu.au

Thus the state of the optical field after the first Hadamard gate is

$$\frac{1}{\sqrt{2}}(|0\rangle+|\alpha\rangle). \tag{2}$$

This is a macroscopic quantum superposition state, often referred to as a cat state. Now consider small changes in path length (i.e. phase shifts) around an integral number of wavelengths (λ) between the two Hadamard gates. Propagation over a distance Δ can be modeled by the unitary operator $\hat{U}(\theta)=\exp(i\theta)\hat{a}^{\dagger}\hat{a}$ where $\theta=2\pi\Delta/\lambda$. The effect of propagation on an arbitrary qubit $|\beta\rangle$, where $\beta=0$ or α, is obtained by examining the overlap

$$\langle\beta|\hat{U}(\theta)|\beta\rangle=\langle\beta|\beta(\cos\theta+i\sin\theta)\rangle$$
$$=\exp[-\beta^2(1-\cos\theta-i\sin\theta)]\approx\exp[i\theta\beta^2], \tag{3}$$

where the approximate final result is true in the limit that the length is small enough that $\theta^2\alpha^2\ll1$ but that α is sufficiently large that $\alpha^2\theta$ is of order 1. Equation (3) implies that under

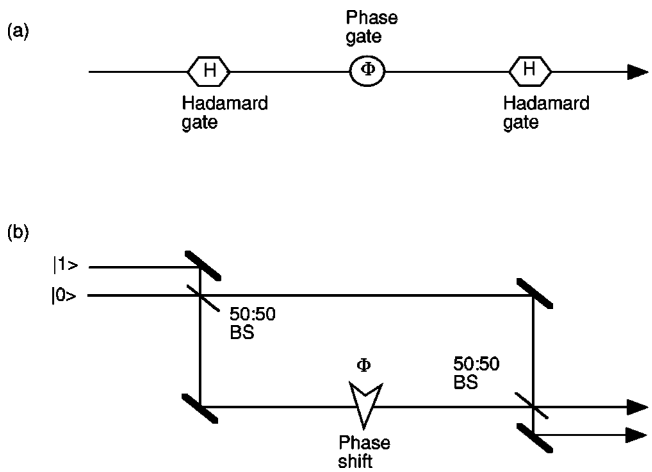

FIG. 1. Schematics of quantum circuit (a) and optical interferometer (b). If a single photon is incident on the interferometer then the description of the path of the photon is mathematically equivalent to the description of the state of the qubit in the quantum circuit with the beam splitters (BS) playing the role of the Hadamards and the phase shift that of the phase gate.

these conditions $\hat{U}(\theta)|\beta\rangle \approx \exp[i\theta\beta^2]|\beta\rangle$ and thus propagation over short distances constitutes a phase gate for this system

$$\hat{U}(\theta)(|0\rangle + |\alpha\rangle) \approx |0\rangle + e^{i\theta\alpha^2}|\alpha\rangle. \tag{4}$$

Hence, the effect of propagation through the entire circuit is given by

$$|\phi\rangle_{out} = \hat{H}\hat{U}(\theta)\hat{H}|0\rangle \approx \tfrac{1}{2}[(1+e^{i\theta\alpha^2})|0\rangle + (1-e^{i\theta\alpha^2})|\alpha\rangle]. \tag{5}$$

Clearly the output state is changed as a function of the propagation distance between the Hadamard gates. We now calculate the sensitivity to that change.

If no perturbation of the length around zero phase shift occurs then the output state will be the vacuum. Thus the signal strength corresponds to the probability of finding the output in the state $|\alpha\rangle$. The measurement noise is the probability that we none the less obtain the vacuum state $|0\rangle$ at the output. The signal-to-noise ratio for measuring small fluctuations in length around zero phase shift is, hence, given by

$$S/N = \frac{\overline{|\langle\alpha|\phi\rangle_{out}|^2}}{|\langle 0|\phi\rangle_{out}|^2} \approx \frac{V_\theta \alpha^4}{4} = V_\theta \overline{n}^2, \tag{6}$$

where the bar indicates a time average and $V_\theta = \overline{|\theta(t)|^2}$ is the time-averaged power in the length fluctuations with $\theta(t)$ taken to be a zero-mean stochastic variable. The average photon number in the cat state between the Hadmard gates is given by $\overline{n} = \alpha^2/2$.

We now compare the sensitivity of the coherent-state quantum circuit to that of a standard interferometer using a squeezed light input. We consider the scheme originally proposed by Caves [10]. A beam in a coherent state with a real amplitude β is injected into one input port of an interferometer whilst a phase-squeezed vacuum is injected into the other input port. We assume the interferometer is balanced (equal path lengths in each arm) and consider the null output port. Small-length fluctuations couple into the phase quadrature of this port. Thus we perform balanced homodyne detection of the phase quadrature X^-, of the null output port. For small-length fluctuations we obtain

$$X^- \approx X_a^+ \frac{\theta}{2} + X_b^-, \tag{7}$$

where X_b^- is the phase (i.e. the squeezed) quadrature of the squeezed vacuum and X_a^+ is the amplitude quadrature of the coherent input. The signal to noise is then given by

$$S/N = \frac{(\beta^2+1)V_\theta}{4V_b^-} \approx \frac{V_\theta \overline{n}^2}{4}, \tag{8}$$

where V_b^- is the noise power in the squeezed quadrature of the squeezed vacuum. In obtaining the final result in terms of the average photon number we have assumed that there is equal power in the coherent beam and the squeezed vacuum and that the squeezed vacuum is strongly squeezed ($V_b^- \ll 1$).

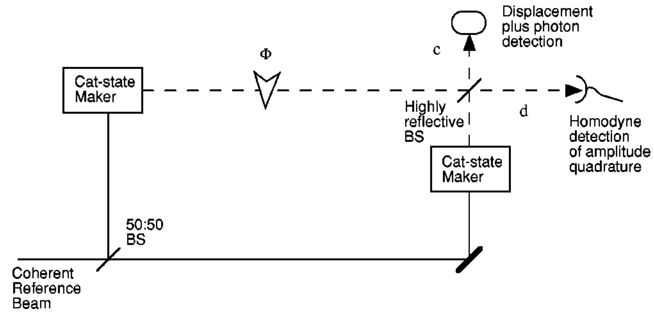

FIG. 2. Schematic of a physical realization of the quantum circuit of Fig. 1(a) using coherent-state encoding. Solid lines are used to indicate coherent beams whilst dashed lines are beams that, in general, are in superposition states.

We see that the signal-to-noise's scale in the same way as a function of photon number for the two systems. This corresponds to an amplitude sensitivity that scales as $1/\overline{n}$, i.e., the Heisenberg limit. Thus both systems perform at the ideal limit set by the uncertainty relations [11]. The factor of 4 increase in signal to noise achieved by the quantum circuit may not be significant. When we examine a particular physical realization later in this paper we will find this advantage disappears.

On the other hand, there is a significant difference in the way the increased sensitivity is reached in the two systems that makes the quantum circuit more versatile. In the squeezed-state interferometer the increase in sensitivity arises from the decrease in background noise in the measurement. However, in the coherent-state circuit the increase is due to a decreasing fringe spacing as the amplitude of the cat is increased. This means, that as α is increased, smaller and smaller length intervals can be resolved with a sensitivity at the Heisenberg limit. This effect is similar to that recently proposed for increasing lithographic resolution [2] and earlier interferometric proposals [12]. Increasing the power in the cat state is effectively the same as increasing the frequency of the light in a standard interferometer, and thus decreasing the fringe spacing. In the earlier proposals increased power also led to the simulation of shorter wavelengths, however, these were based on number state rather than coherent-state superpositions and used quite different manipulations. Other recent schemes for positioning and clock synchronization-type tasks [3,4] are more similar to the squeezed-state interferometer, relying on decreased noise for their increased sensitivity. We believe this quantum-ruler effect could have important applications.

We now consider a physical implementation of our quantum circuit. This is shown schematically in Fig. 2. A coherent-state phase reference beam is divided at a 50:50 beam splitter. One of the beams is sent to a ‘‘generator’’ of macroscopic quantum superposition states of some kind (cat state maker), which produces the state given by Eq. (2), in phase with the reference beam. Such a device is not trivial of course, though some limited success has been achieved in making analogous devices experimentally [13]. Also the cat-state maker need not necessarily be deterministic. In principle, one could imagine building up a resource of the required cat states that are then fed into the interferometer when the measurement is required. A number of nondeterministic schemes for producing cat states have been proposed [14]. These schemes require only linear optics, squeezing, and photon counting for their operation.

The cat-state maker performs the role of the first Hadamard gate in the idealized circuit [Fig. 1(a)]. The cat-state beam is then passed along the path whose distance is to be measured. In order to implement the second Hadamard gate we use the scheme proposed in Ref. [6]. A second cat state, identical to the first, and phase locked to the second coherent reference beam, is weakly mixed with the beam at a highly reflective beam splitter. A surprising result from Ref. [6] is that such a beam splitter, with reflectivity $\cos^2\phi$ where $\phi^2\alpha^2 \ll 1$ but $\phi\alpha^2 = \pi/2$, will act as a control sign gate [15] for our coherent-state qubits. As a result if output state c in Fig. 2 is measured in the "cat basis" (see below) and is found to be in the same cat state as was injected, then the required Hadamard transformation is implemented onto beam d. Alternatively if the output is found in the (near) orthogonal state $1/(\sqrt{2})(|0\rangle - |\alpha\rangle)$, then the output state is a bit-flipped version of the Hadamard gate. The data from the final coherent-state measurement of the output d, is collected in two bins according to the results of the cat-basis measurements.

Notice our physical implementation requires two cat states as resources. Clearly this other resource should be included in calculating the signal to noise in terms of the photon number. The extra factor of 2 will then make the results for the squeezed state and cat schemes equivalent in this realization.

We now introduce explicit models for the measurements. The cat-basis projection would require a high nonlinearity for an exact realization. However, approximate cat-basis measurements can be made by combining displacements and photon-number measurements [6]. The procedure is first displace by $-\alpha/2$. This transforms our 0, α superposition into "$\alpha/2$," "$-\alpha/2$" superposition:

$$D(-\alpha/2)1/\sqrt{2}(|0\rangle \pm |\alpha\rangle) = 1/\sqrt{2}(|-\alpha/2\rangle \pm |\alpha/2\rangle). \quad (9)$$

These new states are parity eigenstates. Thus if photon number is measured then an even result indicates detection of the state $1/\sqrt{2}(|\alpha/2\rangle + |-\alpha/2\rangle)$, and therefore, $1/\sqrt{2}(|0\rangle + |\alpha\rangle)$ whilst similarly an odd result indicates detection of $1/\sqrt{2}(|0\rangle - |\alpha\rangle)$. This measurement technique is different in two major ways from the ideal projection measurement:

(i) If the state being measured is not in just a superposition of $|0\rangle$ and $|\alpha\rangle$, which, in general, will always be true to some extent, then the projective measurement may return a null result, i.e., neither the plus cat or the minus cat. The photon counting technique always returns either an odd or even result.

(ii) The displacement operation prior to photon counting increases the fringe separation by a factor of 2. This effect arises because although $|\alpha\exp[i\theta]\rangle \approx \exp[i\theta\alpha^2]|\alpha\rangle$ we have that

$$D(-\alpha/2)|\alpha\exp[i\theta]\rangle = |\alpha(\exp[i\theta] - 1/2)\rangle \approx \exp[i\theta\alpha^2/2]|\alpha\rangle.$$

This again reduces the prefactor for the sensitivity but does not alter its scaling with photon number. We also replace the final coherent-state projection with the approximately equivalent technique of homodyne detection of the amplitude quadrature.

Having a physical implementation we can now make realistic calculations to confirm the efficacy of the protocol for

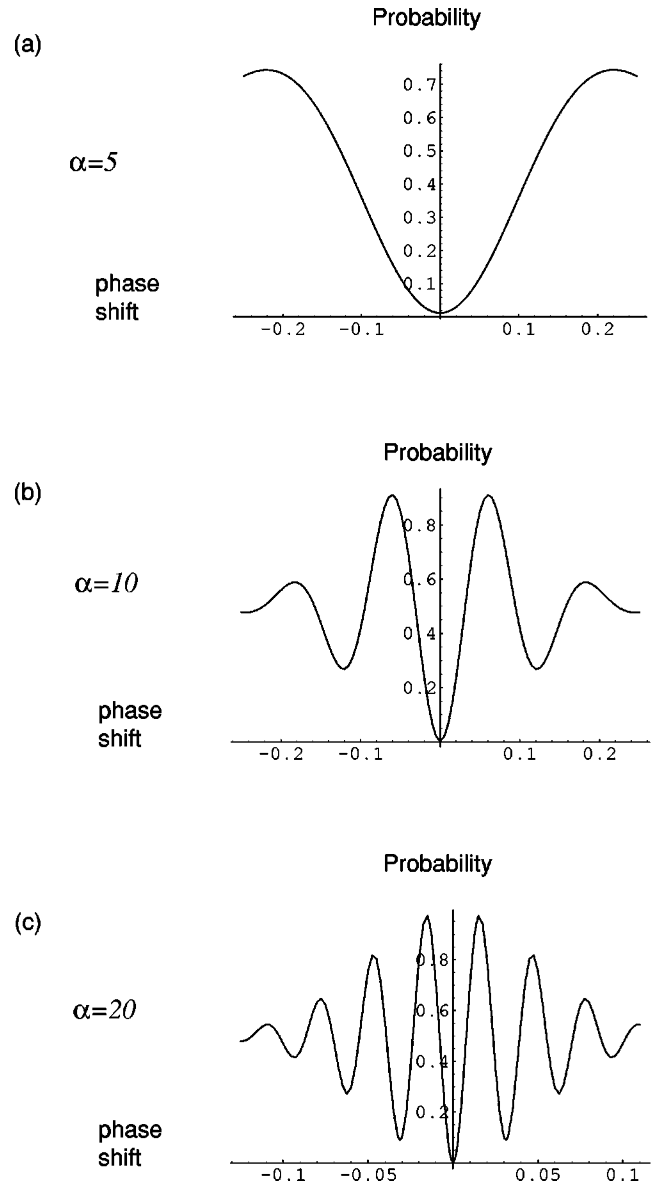

FIG. 3. Probability of obtaining "0" result as a function of the phase shift/distance shift in the interferometer. The coherent amplitude is varied between the three graphs. In (a) $\alpha = 5$, (b) $\alpha = 10$, and (c) $\alpha = 20$. Note that the scale on the horizontal axis of each graph is scaled by $1/\alpha$.

finite values of α. To do this we use the exact solution for the output field for which no assumptions about the magnitude of α have been made. Using the beam-splitter relationship $|\gamma\rangle_a|\beta\rangle_b \rightarrow |\cos\theta\gamma + i\sin\theta\beta\rangle_a|\cos\theta\beta + i\sin\theta\gamma\rangle_b$, a straightforward calculation gives

$$|out\rangle_{\pm} = \frac{1}{2+2e^{-\alpha^2/2}}(A_{\pm}|0\rangle + B_{\pm}|i\alpha\sin(\phi)e^{i\theta}\rangle + C_{\pm}|\alpha\cos\phi\rangle + D_{\pm}|\alpha(\cos\phi + i\sin(\phi)e^{i\theta})\rangle), \tag{10}$$

where

$$A_{\pm} = \langle n_{\pm}| - \alpha/2\rangle,$$

$$B_{\pm} = \langle n_{\pm}|\alpha[\cos(\phi)e^{i\theta} - 1/2]\rangle, \tag{11}$$

$$C_{\pm} = \langle n_{\pm}|\alpha(i\sin\phi - 1/2)\rangle,$$

$$D_{\pm} = \langle n_{\pm}|\alpha(\cos\phi + i\sin(\phi)e^{i\theta} - 1/2)\rangle,$$

and $\phi = \pi/(2\alpha^2)$ and an even (odd) number n_+ (n_-) of photons have been counted. The state overlaps can be calculated using the relationship [16] $\langle n|\alpha\rangle = \exp[-|\alpha|^2/2]\alpha^n/\sqrt{n!}$. We then calculate

$$P_{\pm} = \frac{1}{\sqrt{\pi}}\int_{-\infty}^{\alpha/2}|\langle x'|out\rangle_{\pm}|^2 dx', \tag{12}$$

where $\psi_{out} = \langle x'|out\rangle_{\pm}$ is the amplitude quadrature wave function of the output field and can be calculated using

$$|\langle x'|\gamma\rangle|^2 = \exp\left[-\left(\frac{\gamma+\gamma^*}{2} - x'\right)^2\right]. \tag{13}$$

Equation (12) gives the probability that a measurement of the amplitude quadrature of output beam *d* gives a result lying below $\alpha/2$. This we consider a "0" result. When an even number of photons is counted at output *c* we label this result P_+. When an odd number of photons is found at output *c* we label the result P_-. The two probabilities show fringes as a function of θ but they are $\pi/2$ out of phase. Note that this means that without the cat-basis measurements to distinguish the two cases the fringes would be completely washed out.

With the cat-basis binning of the results we are able to form the following function: $(\Sigma_{n_-}P_- - \Sigma_{n_+}P_+ + 1)/2$, which corrects for the bit flip between the results and now sums over all photon numbers. This is evaluated numerically and plotted for various values of α in Fig. 3. The width of the middle fringe scales as $1/\alpha^2$ between the three graphs (note changing axis scale). This indicates sensitivity at the Heisenberg limit.

The quantum ruler effect is also clear. As α increases, a number of high visibility, narrowly spaced fringes emerge. The fringe spacing is as expected for the parity measurement scheme. The fringes could enable very short-length intervals to be accurately measured. As an example suppose our laser wavelength is 1 μm. In a standard interferometer this would enable length intervals of 0.5 μm to be stepped off. The use of squeezing would increase the precision of our measurements but would not change the length scale. However, using the cat-state interferometer with an α of 20 [Fig. 3(c)] leads to the fringe separation being reduced to 3.3 nm.

We have introduced an interferometer based on a recently discussed quantum circuit for coherent states and their superposition. We have shown that this arrangement has a sensitivity at the Heisenberg limit and also displays a quantum ruler effect that could be used to resolve precisely very small length intervals. This work highlights the different mechanisms at play between squeezing and quantum-circuit metrology. The present analysis does not consider imperfections in the cat-state resources, optical networks or detectors. Due to the fragility of large cat states [16] it is likely that the interferometer would have very low tolerances to such imperfections. The experiments suggested here would thus be extremely technologically demanding for large α. None the less it is of considerable interest that, in principle, only linear optics, squeezed sources, and photon counting is required for a demonstration. As well as possible applications in metrology the experiments suggested here may also serve as an initial testing ground for coherent-state quantum circuits.

We acknowledge useful discussions with G. J. Milburn and W. J. Munro. This work was supported by the Australian Research Council.

[1] G. J. Milburn, Phys. Rev. Lett. **62**, 2124 (1988).
[2] A. N. Boto, P. Kok, D. S. Abrams, S. L. Braunstein, C. P. Williams, and J. P. Dowling, Phys. Rev. Lett. **85**, 2733 (2000).
[3] V. Giovannetti, S. Lloyd, L. Maccone, and F. N. C. Wong, Phys. Rev. Lett. **87**, 117902 (2001).
[4] V. Giovannetti, S. Lloyd, and L. Maccone, e-print quant-ph/0107140.
[5] W. J. Munro, K. Nemoto, G. J. Milburn, and S. L. Braunstein, e-print quant-ph/0109049.
[6] T. C. Ralph, W. J. Munro, and G. J. Milburn, e-print quant-ph/0110115.
[7] P. T. Cochrane, G. J. Milburn, and W. J. Munro, Phys. Rev. A **59**, 2631 (1999).
[8] H. Jeong and M. S. Kim, e-print quant-ph/0109077.
[9] D. A. Rice, G. Jaeger, and B. C. Sanders, Phys. Rev. A **62**, 012101 (2000).
[10] C. M. Caves, Phys. Rev. D **23**, 1693 (1981).
[11] W. Heitler, *The Quantum Theory of Radiation* (Oxford University Press, Oxford, 1954).
[12] M. J. Holland and K. Burnett, Phys. Rev. Lett. **71**, 1355 (1993).
[13] C. Monroe, D. M. Meekhof, B. E. King, and D. J. Wineland, Science **272**, 1131 (1996); M. Brune, E. Hagley, J. Dreyer, X. Maitre, A. Maali, C. Wunderlich, J. M. Raimond, and S.

Haroche, Phys. Rev. Lett. **77**, 4887 (1996); Q. A. Turchette, C. J. Hood, W. Lange, H. Mabuchi, and H. J. Kimble, *ibid.* **75**, 4710 (1995).

[14] S. Song, C. M. Caves, and B. Yurke, Phys. Rev. A **41**, 5261 (1990); M. Dakna, T. Anhut, T. Opatrny, L. Knll, and D.-G. Welsch, *ibid.* **55**, 3184 (1997).

[15] A control sign gate produces the following logic table: $|0\rangle_L|0\rangle_L \rightarrow |0\rangle_L|0\rangle_L$, $|0\rangle_L|1\rangle_L \rightarrow |0\rangle_L|1\rangle_L$, $|1\rangle_L|0\rangle_L \rightarrow |1\rangle_L|0\rangle_L$ but $|1\rangle_L|1\rangle_L \rightarrow -|1\rangle_L|1\rangle_L$.

[16] D. F. Walls and G. J. Milburn, *Quantum Optics* (Springer-Verlag, Berlin, 1994).